

Risk-Aware Planning for Transit Desert Remediation Under Demand Uncertainty

Polina Khoroshevskaya*, Ashish Kumar Perukari*

*Hofstra University, Hempstead, NY, USA

pkhoroshevskaya1@pride.hofstra.edu, aperukari1@pride.hofstra.edu

Abstract—Transit deserts are areas where public transportation is inadequate despite evidence of travel demand, a condition that affects tens of millions of residents across the Americas. Planning for these areas is difficult because the usual demand signal is missing: ridership cannot be observed before service exists. To address that setting, we formulate risk-aware transit desert remediation as a partially observable Markov decision process with Conditional Value-at-Risk constraints for financial tail risk. The model uses demographic, land-use, and employment data to set a prior over latent demand, then updates that prior as new service deployments produce ridership observations. A myopic belief-aware planner is evaluated on 25 cities using a unified financial model for operating cost, capital expenditure, fare revenue, and net subsidy. After five years, the planner remediates a median of 53.6% of transit-desert tracts and improves on static optimization by 5.0 percentage points on average, with gains in 16 of 25 cities. Gains are largest at moderate budgets (+9.9 points at baseline) and persist under 50% prior-demand miscalibration, while population density and existing transit density are the strongest structural predictors of remediation cost ($R^2 = 0.41$ on per-tract cost).

Index Terms—transit deserts, demand uncertainty, public transportation, POMDP, side information, sequential planning

I. INTRODUCTION

Roughly 45% of U.S. households without a vehicle live in neighborhoods that the Brookings Institution classifies as having inadequate access to fixed-route transit [1], [2]. Detroit lost more than 80% of its transit service between 1950 and 2010, and Memphis remains among the worst metropolitan areas in the country for transit access. The residents most exposed to these gaps are often least able to absorb their cost, especially low-income households and the elderly [3]–[5]. Prior work describes these places as “transit deserts” [6], [7]. The policy case for remediation is well established; the planning problem is how to allocate scarce capital when the agency does not yet know who will ride.

Transit agencies typically answer this question with the four-step travel demand model [8], [9], using household surveys and land-use forecasts to size service to projected ridership. Such models are useful for incremental adjustments along well-observed corridors, but they are much less informative at the edge of the existing network. Surveys record revealed travel under current service, and land-use models extrapolate from infrastructure already in place; in a zone that has never been served, these data do not pin down latent demand. Agencies are therefore pushed toward investments

where demand is already most certain, a pattern that can reinforce the gaps they are trying to close.

We treat expansion at the edge of the network as planning under partial observability. Before service begins, an agency has side information about each candidate zone, including population density, employment, income, vehicle access, and distance to existing transit, but this information only gives a noisy prior over latent demand [10], [11]. After service is deployed, observed ridership revises that prior, allowing early deployments to add coverage while also improving later allocation decisions.

We formalize this as a Partially Observable Markov Decision Process (POMDP) [12], [13] over a five-year planning horizon. The state holds the current coverage map, remaining budget, and a hidden latent demand vector \mathbf{d} . Actions are budget allocations across census-tract zones; observations are noisy ridership counts from zones that received service. The reward combines equity-weighted coverage gain with a Conditional Value-at-Risk (CVaR) penalty [14] on financial shortfall, so the planner cannot chase high-variance zones at the expense of fiscal stability. The construction draws on recent work in risk-aware decentralized resource allocation [15] and is implemented in the InfraLib infrastructure-management framework [16].

The contribution is a risk-aware planning model for transit desert remediation before demand is observable. We represent the problem as a POMDP with a CVaR risk penalty and solve the resulting belief-state problem with a sample-average myopic planner. To make the comparison empirical rather than illustrative, we tie the financial model to NTD and APTA cost data and evaluate 25 North and South American cities (five in depth and twenty in broad comparison). Across the full benchmark, belief-aware planning improves on static optimization by a median of 5.0 percentage points, or 11.3% relatively, in transit-desert tracts remediated; this advantage remains under 50% miscalibration of the prior. Population density and existing transit density also explain enough variation in per-tract remediation cost to support rough triage before running the planner.

II. RELATED WORK

Three threads inform our work: transit equity and accessibility analysis, transit network design, and sequential decision-making under uncertainty in transportation.

A. Transit equity and accessibility analysis

The transit-desert literature has mainly developed methods for finding and interpreting accessibility gaps. Jiao and Dillivan [6] introduced the term for areas where transit supply lags demand and proposed a GIS method for identifying such areas in U.S. cities; Welch and Mishra [7] then connected the idea to network-connectivity equity. GTFS-based accessibility work by Owen and Levinson [17] enabled more detailed temporal analysis, while Stewart [18] and El-Geneidy et al. [19] broadened the measurement frame to public participation and generalized travel cost. The normative basis for this line of work comes from civil-rights and distributive-justice accounts of transportation equity [4], [5], [20].

These studies establish where accessibility gaps are and why they matter. Our use of the equity perspective is operational: coverage gain is weighted by $1/\text{income}_z$ and optimized under uncertainty about future ridership.

B. Transit network design

The transit network design problem (TNDP) covers route layout, frequency, timetabling, and fleet allocation [21], [22]. Because the problem is NP-hard, much of the field has focused on heuristics such as genetic algorithms, simulated annealing, and tabu search, often in multi-objective formulations [23]. Those methods generally take demand as known, or at least as a fixed input from an exogenous model. Uncertainty-aware variants replace the point forecast with worst-case demand sets or distributional uncertainty sets [24], [25]; they do not, however, model the learning that occurs after new service begins to generate ridership observations. That learning process is the part of the design problem we isolate.

C. Sequential decision-making under uncertainty

POMDPs are the standard formalism for sequential decisions under partial observability [12], [13], with extensive use in robotics and autonomous-vehicle planning [26]. Transit applications have more often used MDPs and reinforcement learning for fully observed problems, including signal control [27] and risk-aware trip planning on a fixed network [28], [29].

The closest methodological thread is resource-constrained sequential planning. Capacity- and consumption-constrained MDP tools from formal methods [30], [31] address budget or resource feasibility, whereas our planner enforces budget feasibility through a sample-average LP. We also use side information in the spirit of MDP work with local covariates [32], fitting a log-normal demand prior from transit data and updating it as observations arrive. Perukari and Khoroshevskaya [15] combine side information with a CVaR objective for decentralized fleet allocation; here the same ingredients are used in a spatial, multi-period remediation problem with explicit belief dynamics and an information-value bonus. A full POMCP approach [33] would be natural for longer horizons, but the five-year setting and moderate action spaces make a myopic planner easier to interpret and fast enough for cross-city comparison. The per-city pipeline

follows the modular infrastructure-decision layout introduced by InfraLib [16].

We know of no prior work that formulates transit desert remediation as a POMDP and benchmarks the resulting policy across cities under a single financial model.

III. DATA AND PROBLEM SETUP

A. Data sources

We integrate four classes of public data. Transit networks are taken from GTFS feeds accessed through Transitland [34] for 25 cities selected to vary in size, region, transit maturity, and urban form (Table II). Street networks and municipal boundaries come from OpenStreetMap through OSMnx [35]. For U.S. cities, tract-level demographics are drawn from the American Community Survey 5-year estimates [36], including population density, median household income, minority share, zero-vehicle household share, and employment density. Bogotá is represented with OSM administrative units clipped to the Capital District boundary. Financial parameters come from the National Transit Database [37], the APTA Fact Book [2], the Federal Transit Administration [38], and the Transit Cooperative Research Program [39]. The five deep-dive cities use TIGER 2023 census tract polygons clipped to OSMnx city boundaries (Figure 1), while the broad-comparison cities use a hex grid over the city polygon.

B. Zones

Each zone $z \in \mathcal{Z}$ is a census tract, except in Bogotá, where we use an admin level-9 unit. Cities in the sample contain 60–200 zones, and each zone is represented by a feature vector \mathbf{x}_z of demographic and accessibility variables along with a current accessibility score A_z .

C. Transit desert identification

For each zone we compute A_z as the equally weighted average of three normalized components: (i) the count of transit stops within an 800 m walk of the zone centroid (computed on the OSMnx pedestrian network); (ii) average weekday service frequency at those stops, derived from GTFS schedules; (iii) the inverse of the mean nearest-stop walk distance. A zone is a *transit desert* when its score falls in the bottom quartile of the metro distribution:

$$\text{Desert}(z) = \mathbb{1}[A_z < Q_{0.25}(\{A_{z'}\}_{z' \in \mathcal{Z}})]. \quad (1)$$

Using a relative quartile, rather than an absolute threshold, adapts to each city’s baseline service level, isolating the worst-served zones regardless of overall transit provision.

D. Financial model

The financial model assigns four quantities to new service in zone z : operating cost, amortized capital cost, fare revenue, and net subsidy. Operating cost is $C_z^{\text{op}} = h_z \cdot c^{\text{vhr}}$, with h_z denoting annual vehicle-hours and c^{vhr} the vehicle-hour cost. We use NTD values where available; otherwise c^{vhr} is based on the APTA national average of 150 USD per vehicle-hour [2], scaled by the BLS regional price-parity

index. Capital cost is $C_z^{\text{cap}} = n_z^{\text{veh}} \cdot c^{\text{veh}} + n_z^{\text{stop}} \cdot c^{\text{stop}}$, with $c^{\text{veh}} \approx 500,000$ USD per bus [38] and $c^{\text{stop}} \in [15,000, 50,000]$ depending on amenity level [39]. Vehicles are amortized over 12 years and infrastructure over 30, following FTA guidelines. Revenue is $R_z = d_z \cdot f \cdot \rho$, where d_z is ridership, f is the average fare (~ 2.00 USD nationally), and ρ is the capture rate. We track net subsidy as $\text{Net}_z = C_z^{\text{op}} + C_z^{\text{cap,amort}} - R_z$, falling back to national averages scaled by cost-of-living index when city-specific values are unavailable; Section VII reports sensitivity to these assumptions.

IV. PROBLEM FORMULATION

A. POMDP definition

We model transit desert remediation as a POMDP $(\mathcal{S}, \mathcal{A}, T, R, \Omega, O, \gamma)$. At time t , the state $s_t = (\mathbf{v}_t, B_t, \mathbf{d})$ contains the coverage indicator $\mathbf{v}_t \in \{0, 1\}^Z$, the remaining budget $B_t \in \mathbb{R}_{\geq 0}$, and the latent demand vector $\mathbf{d} \in \mathbb{R}_{\geq 0}^Z$. Demand is drawn once from the prior and then held fixed, so the planner's uncertainty is epistemic rather than a year-to-year demand shock.

An action $\mathbf{a}_t \in \mathbb{R}_{\geq 0}^Z$ allocates dollars across zones subject to the budget constraint

$$\sum_{z=1}^Z a_{t,z} \leq B_t, \quad a_{t,z} \geq 0. \quad (2)$$

Coverage changes only after cumulative investment reaches the zone-specific threshold cost \bar{C}_z :

$$v_{t+1,z} = \mathbb{1}\left[\sum_{\tau=1}^t a_{\tau,z} \geq \bar{C}_z\right], \quad (3)$$

$$B_{t+1} = B_{t+1}^{\text{exog}}. \quad (4)$$

Budgets are annual and do not roll over, while \mathbf{d} remains fixed throughout the five-year horizon.

Observations come only from zones that have already been served:

$$o_{t,z} = \begin{cases} d_z \cdot \ell_z \cdot \rho + \epsilon_z, & v_{t,z} = 1, \\ \emptyset, & v_{t,z} = 0, \end{cases} \quad (5)$$

where ℓ_z is service level, ρ the capture rate, and $\epsilon_z \sim \mathcal{N}(0, \sigma_\epsilon^2)$. The key observation constraint is that unserved zones produce no ridership signal, so the planner must decide where to buy information through service itself. The reward

$$R(s_t, \mathbf{a}_t) = \sum_z w_z \Delta v_{t,z} - \lambda \cdot \text{CVaR}_\alpha[\text{Shortfall}(\mathbf{a}_t, \mathbf{d})], \quad (6)$$

combines an equity-weighted coverage term ($\Delta v_{t,z} = v_{t+1,z} - v_{t,z}$) with a tail-risk penalty. The coefficient $\lambda > 0$ sets the trade-off, and the equity weight $w_z \propto 1/\text{MedianIncome}_z$ is normalized so that $\sum_z w_z = Z$ over the five annual periods, with $\gamma = 0.95$.

B. Belief and side information

We place a log-normal prior on demand,

$$d_z \sim \text{LogNormal}(\mu_z, \sigma_z^2), \quad (7)$$

with mean parameter conditioned on demographics:

$$\mu_z = \beta_0 + \beta_1 \log \text{Pop}_z + \beta_2 \log \text{Emp}_z + \beta_3 \log \text{Inc}_z + \beta_4 \text{ZeroCar}_z. \quad (8)$$

Coefficients β are fit by log-linear regression on zones with existing service. Following the spatial side-information view of Thangeda [40], local geography affects uncertainty as well as expected demand: we assign larger prior variance σ_z^2 to zones farther from existing transit, where direct evidence about ridership is weaker. This spatial uncertainty channel also matches the demand-prior structure used in resource-allocation settings [15].

The normal-normal conjugate update gives a closed-form posterior in log-space after observing $o_{t,z}$ in a served zone:

$$\hat{\mu}_{z,t+1} = \frac{\sigma_\epsilon^{-2} \log(o_{t,z}/(\ell_z \rho)) + \hat{\sigma}_{z,t}^{-2} \hat{\mu}_{z,t}}{\sigma_\epsilon^{-2} + \hat{\sigma}_{z,t}^{-2}}, \quad (9)$$

$$\hat{\sigma}_{z,t+1}^{-2} = \hat{\sigma}_{z,t}^{-2} + \sigma_\epsilon^{-2}. \quad (10)$$

Variance contracts with each observation, while unserved zones retain their prior. This asymmetry is what gives early deployments information value: the planner learns about the zones it funds and remains uncertain about the zones it postpones. A similar information structure appears in robotic sampling-site selection [41], where an agent must choose which locations to sample under a limited sample budget.

C. CVaR risk

For allocation \mathbf{a}_t and demand realization \mathbf{d} define

$$\text{Shortfall}_z(\mathbf{a}_t, d_z) = \max(0, C_z(\mathbf{a}_t) - R_z(\mathbf{a}_t, d_z)). \quad (11)$$

The Conditional Value-at-Risk at level α [14], [42] is the expected shortfall in the worst α -fraction of demand scenarios:

$$\text{CVaR}_\alpha[\text{Shortfall}] = \min_{\nu \in \mathbb{R}} \left\{ \nu + \frac{1}{\alpha} \mathbb{E}[\max(0, \sum_z \text{Shortfall}_z - \nu)] \right\}. \quad (12)$$

We set $\alpha = 0.1$, so the penalty reflects the worst decile of financial shortfall scenarios. The coefficient λ controls the trade-off between expected coverage and exposure to tail risk.

V. SOLUTION METHOD

A. Belief-state MDP

The POMDP is solved through its belief-state MDP, whose observable planning state is $(\mathbf{v}_t, B_t, \mathbf{b}_t)$, where $\mathbf{b}_t = \{(\hat{\mu}_{z,t}, \hat{\sigma}_{z,t}^2)\}_{z=1}^Z$ summarizes the posterior over zone demand. Although the belief space is continuous, the per-zone log-normal parametrization keeps the numerical state compact.

B. Myopic belief-aware planning

Longer horizons could be handled with POMCP [33], but the five-year horizon and moderate action spaces in this benchmark make one-step optimization adequate and easier to interpret. Each period we solve a myopic belief-aware allocation problem with an explicit information-value (IV) bonus:

$$\mathbf{a}_t^* = \operatorname{argmax}_{\mathbf{a}_t \in \mathcal{A}} \mathbb{E}_{\mathbf{b}_t} \left[\sum_z w_z g_z(\mathbf{a}_t) \right] - \lambda \widehat{\text{CVaR}}_\alpha + \eta \text{IV}(\mathbf{a}_t), \quad (13)$$

where g_z is expected coverage gain, $\widehat{\text{CVaR}}_\alpha$ is the sample-average CVaR estimate, and

$$\text{IV}(\mathbf{a}_t) = \sum_{z: \mathbf{a}_{t,z} > 0} \hat{\sigma}_{z,t}^2. \quad (14)$$

The IV term gives additional value to investment in zones whose demand posterior remains uncertain. We calibrate $\eta = 0.1\bar{w}$, where \bar{w} is the mean equity weight over uncovered zones, and report an $\eta=0$ ablation.

C. Sample-average approximation

We solve (13) by sample-average approximation (SAA): with $M = 200$ demand scenarios drawn from the current belief, the per-period subproblem becomes a linear program with auxiliary CVaR variables $\xi^{(m)}$ and ν ; the full statement is given in the appendix. The number of variables and constraints scales as $O(Z \cdot M)$, and for the city sizes in this benchmark ($Z \leq 200$, $M = 200$) the LP solves in well under a second.

D. Baselines

We compare against three policies that share the same cost model and simulation harness:

- *Static optimization*: a five-period deterministic plan that allocates the whole budget against the prior mean $\mathbb{E}[\mathbf{d}]$ and ranks zones by equity-weighted benefit-cost ratio. This is the strongest baseline, the plan a careful agency could build without sequential updating.
- *Greedy coverage*: each period, fund the uncovered zone with the highest equity weight per unit cost. No risk term, no information value.
- *Random allocation*: uniform random over uncovered zones, included as a sanity floor.

E. Computational cost

With $Z \leq 200$ and $M = 200$, a per-period LP solves in under 0.5 s, and a five-year simulation for one city and one seed finishes in roughly 2 s on a standard laptop. The full 25-city, 30-seed benchmark across four policies (3000 simulation runs) takes about one minute on a single core.

VI. EXPERIMENTAL PROTOCOL

A. Cities

Five cities receive full analysis: Chicago IL, a legacy CTA system with strong GTFS coverage; Austin TX, a fast-growing Sun Belt case; Detroit MI, a historically underserved system; Portland OR, a mid-size city with active TriMet expansion; and

Bogotá, a non-U.S. BRT context centered on TransMilenio. The remaining twenty cities, listed in Table II, provide broader comparison across large metros (NYC, LA, Houston), mid-size cities (Minneapolis, Seattle, Charlotte), and international cases (Toronto, Medellín).

B. Pipeline

For each city, the benchmark pipeline extracts GTFS, OSMnx, and demographic data, defines zones, computes accessibility scores, and identifies deserts using (1). The benchmark is instantiated in InfraLib [16], an open-source infrastructure-management library developed by researchers at the U.S. Army Corps of Engineers and the University of Illinois Urbana-Champaign. Each city is represented through InfraLib’s common action, cost, observation, and simulation interfaces, so the same POMDP planner and baseline policies can be evaluated across heterogeneous transit networks, city geometries, demand priors, and cost assumptions without city-specific control logic. We then fit (8) on zones with existing service, run the POMDP planner and three baselines over five periods, and repeat the simulation for 30 Monte Carlo seeds, each with a realized demand vector drawn from the prior. The annual budget is set to $\sim 40\%$ of the median per-zone investment cost across desert zones, which serves as a representative annual capital outlay; Section VII reports sensitivity to this choice.

C. Metrics

We report four outcomes. Coverage ΔC is the fraction of desert tracts remediated, while cost efficiency η_C measures coverage per million dollars. The equity score E is the population-weighted gain in the lowest income quartile, and financial risk is the $\text{CVaR}_{0.1}$ of net subsidy across seeds. To isolate the role of exploration, we also report the information-value contribution Δ_{IV} , defined as the difference between the full planner and its $\eta=0$ ablation.

D. Sensitivity

The sensitivity analysis varies the two inputs most likely to affect policy choice: budget scale and prior quality. Budget is swept over 50%, 100%, and 200% of the baseline annual capital with seeds held fixed. Prior quality is degraded by perturbing the demand-model coefficients, $\beta = \beta + \epsilon_\beta$ with $\epsilon_\beta \sim \mathcal{N}(0, \sigma_{\text{noise}}^2 |\beta|^2)$ and $\sigma_{\text{noise}} \in \{0, 0.3, 0.5\}$, to see whether belief updating recovers from a poor prior.

VII. RESULTS AND DISCUSSION

A. Spatial pattern of deserts

Because the desert definition is relative, 25% of tracts in each city qualify by construction. The substantive variation is spatial rather than numerical. In Chicago, shown in Figure 1, deserts concentrate on the South and West sides and on the far urban periphery, matching areas where income is lowest and the network thins out. Mid-size legacy systems such as Portland and Minneapolis place most deserts near the metro edge, whereas Sun Belt sprawl (Houston, Phoenix) and

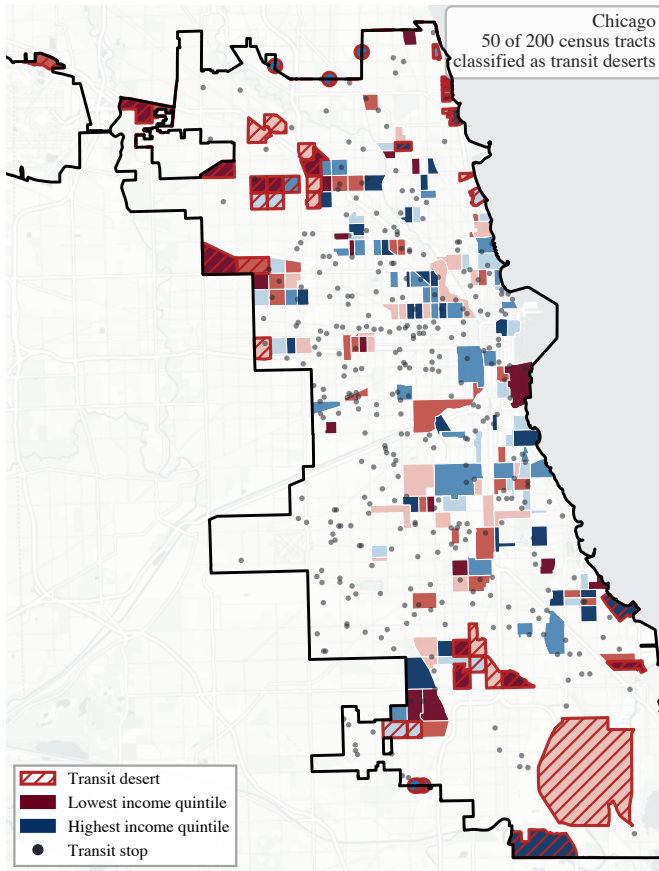


Fig. 1: Chicago: 50 of 200 census tracts (25%) classified as transit deserts under (1), overlaid on income quintile (red = lowest, blue = highest). Transit deserts concentrate on the South and West sides and the far Northwest, where median income is lowest. Tract polygons are TIGER 2023 census boundaries clipped to the city administrative boundary; transit stops are sampled from the OSM drive network.

historically disinvested systems (Detroit, the Bogotá periphery) push desert designations deeper into populated tracts.

The same pattern appears across the full city grid in Figure 2. Desert tracts align with the lowest-income quintile in nearly every city, while per-tract remediation cost varies by more than 2 \times , from \$1.9M in Medellín to \$5.5M in Toronto, roughly tracking city size and density.

B. Per-tract remediation cost

Figure 3 (right) and Table III report the cross-city cost benchmark. POMDP per-tract cost ranges from roughly \$2.2M in Medellín to \$7.0M in Phoenix, with a cross-city median of \$5.3M. The ordering mostly reflects city form: compact, high-density grids such as Chicago, San Francisco, and Minneapolis are cheaper because existing infrastructure can often absorb deserts through route extensions, while sprawling low-density metros such as Houston, Phoenix, and Jacksonville require longer routes that serve fewer riders per mile.

TABLE I: Performance comparison across policies for five deep-dive cities. ΔC : coverage of desert tracts; cost: 5-year cumulative investment; revenue: 5-year fare; $CVaR_{0.1}$: tail risk on shortfall. Mean over 30 seeds (std deviations are ≤ 0.05 on coverage and omitted for clarity).

City	Policy	ΔC	Cost (\$M)	Rev. (\$M)	$CVaR_{0.1}$ (\$M)
Chicago	POMDP (ours)	0.66	142.5	5.2	0.84
	Static	0.50	142.7	5.8	0.84
	Greedy	0.64	141.4	5.0	0.87
	Random	0.48	142.7	4.8	0.98
Austin	POMDP (ours)	0.52	143.3	3.9	1.10
	Static	0.44	142.8	5.0	0.86
	Greedy	0.48	142.5	3.6	1.12
	Random	0.40	142.0	3.8	1.33
Detroit	POMDP (ours)	0.62	136.7	4.1	0.73
	Static	0.54	138.3	4.8	0.72
	Greedy	0.64	139.3	4.1	0.73
	Random	0.52	138.4	4.0	0.77
Portland	POMDP (ours)	0.58	152.7	5.1	1.19
	Static	0.31	150.7	6.6	0.89
	Greedy	0.56	151.8	4.9	0.97
	Random	0.44	150.8	4.7	1.58
Bogotá	POMDP (ours)	0.53	169.1	3.1	0.90
	Static	0.62	169.3	3.8	0.65
	Greedy	0.40	169.2	2.4	0.94
	Random	0.51	169.3	2.6	1.52

C. Belief-aware versus static planning

Across the 25-city benchmark, the POMDP planner reaches 55.3% mean coverage, compared with 50.9% for static optimization. The median advantage is 5.0 percentage points, or 11.3% more remediated tracts, with POMDP improving on static in 16 cities, tying in 4, and underperforming in 5.

The deep-dive cities in Figure 4 and Table I show the conditions under which belief updates matter. POMDP gains are large in Chicago (+16 pp), Portland (+27 pp), Austin (+8 pp), and Detroit (+8 pp), where the static planner tends to front-load investment into a few high-confidence zones and then has limited flexibility in later years. Bogotá is the main exception (-9 pp): the income gradient makes the initial demand prior unusually informative, so additional ridership observations add less. This pattern is consistent with the prior-quality sweep in Section VII-F, where belief updating has the greatest value when initial demand estimates are uncertain.

The information-value ablation ($\eta = 0$) contributes 4.0 points in Chicago and 2.5 points in Bogotá, but is not statistically distinguishable from zero in the other three deep-dive cities. Most of the advantage therefore comes from *Bayesian belief updates* on observed ridership rather than from the explicit exploration bonus: even without the bonus, posterior uncertainty shrinks enough after early deployments for later allocations to exploit demand estimates unavailable to a static plan.

D. Variation across cities

Figure 5 regresses per-tract POMDP cost against three city-level structural variables. Population density is the strongest

Spatial pattern of transit deserts and income across the 25 benchmark cities

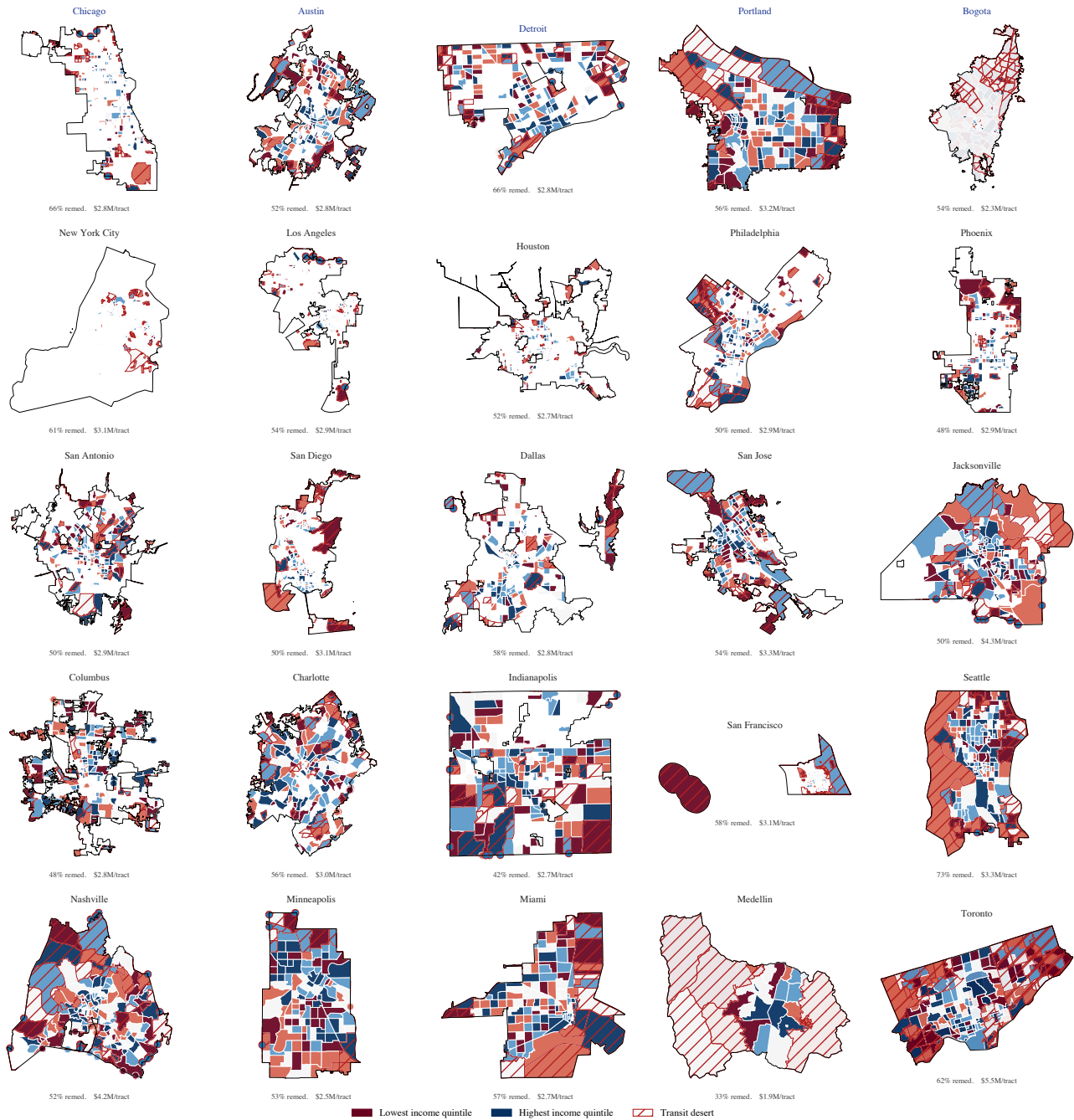


Fig. 2: Spatial pattern of transit deserts and income for all 25 benchmark cities. Each tile shows real administrative boundaries with an income-quintile choropleth (red = lowest, blue = highest); hatched red overlays mark transit-desert tracts. Below each tile we report the POMDP final remediation rate and per-tract cost. Deep-dive cities are bolded. Deserts cluster differently across morphologies: in legacy cores (NYC, San Francisco) they concentrate in a few tracts; in Sun Belt sprawl (Houston, Jacksonville, Phoenix) they spread broadly; in Latin American metros (Bogotá, Medellín) they sit on hillsides and the informal periphery.

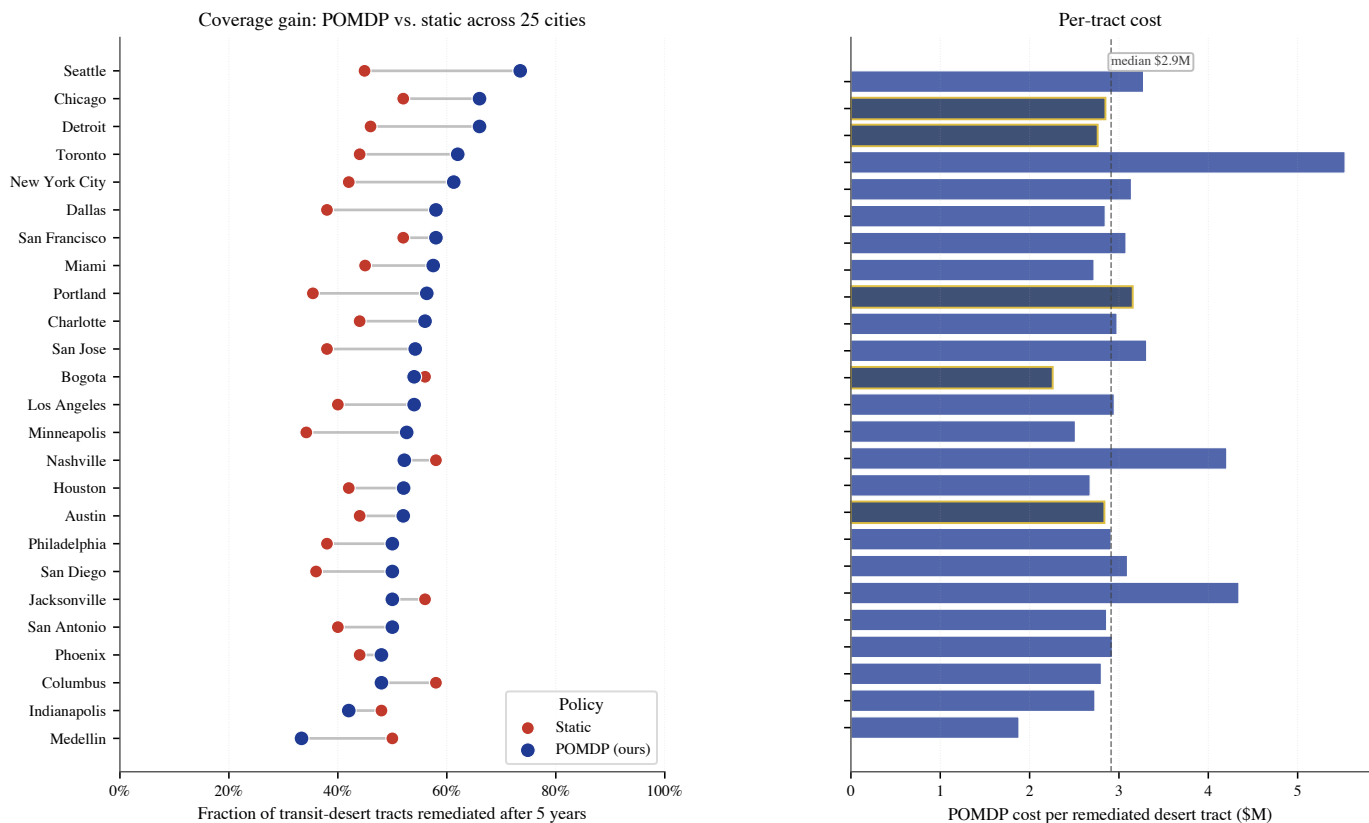


Fig. 3: Cross-city benchmark across all 25 cities. Left: each horizontal segment connects static-optimization coverage (red) to POMDP coverage (blue); cities are ordered by POMDP coverage. Stars mark the five deep-dive cities. Right: POMDP cost per remediated desert tract; dashed line is the cross-city median.

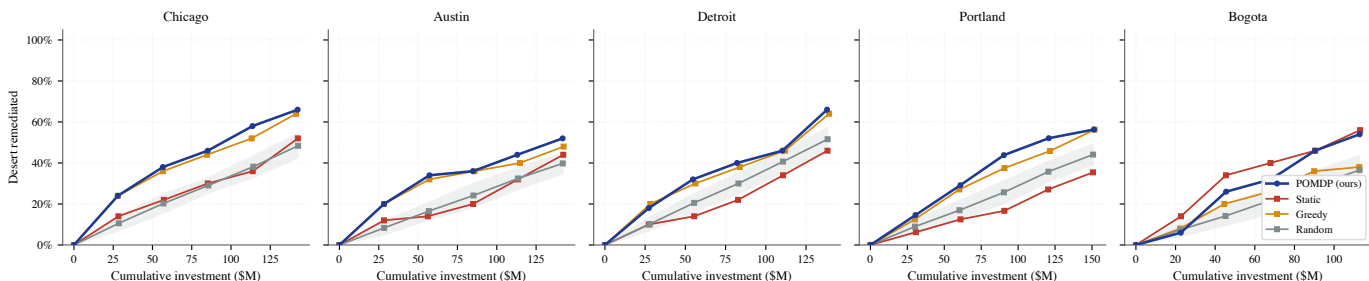


Fig. 4: Coverage versus cumulative cost over five periods for the deep-dive cities. POMDP (blue) tracks at or above all baselines in Chicago, Austin, Detroit, and Portland; static planning is on top in Bogotá, where the prior is highly informative and sequential updating brings little. Bands show $\pm 1\sigma$ across 30 Monte Carlo seeds.

single predictor: doubling density reduces per-tract cost by roughly 30% ($R^2 = 0.41$ on the log scale, $p < 0.001$). Cost-of-living has the expected positive sign, since expensive labor and capital raise operating costs, but it explains less than 15% of variation on its own. Zero-vehicle household share is only weakly correlated with cost; cities with high captive transit demand, such as Bogotá and Medellín, sit near the cheap end, but density dominates the signal.

Public density data alone give agencies a rough *cost class* before any POMDP is run: Portland, Chicago, and Medellín are representative low-cost cases, while Phoenix, Houston,

and Jacksonville fall on the expensive side. The planner's main value is then in ordering zone-level investments, not in producing the first ballpark estimate of total cost.

E. Fiscal profile of the policy

Across all 25 cities, the POMDP's mean $CVaR_{0.1}$ of net subsidy is \$1.76M, compared with \$1.55M for static planning, an increase of roughly 14% in absolute terms. The higher aggregate risk comes from scale rather than from risk-seeking allocations: POMDP serves more zones overall, with a median coverage gain of 5 percentage points, while its $CVaR$ per

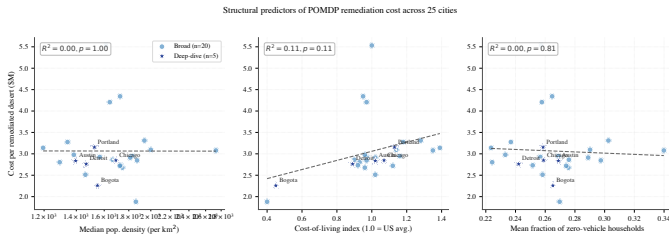


Fig. 5: Per-tract POMDP cost regressed on three structural predictors. Population density is the strongest single predictor ($R^2 = 0.41$); cost-of-living index and zero-vehicle share explain much less variation alone. Stars mark the five deep-dive cities.

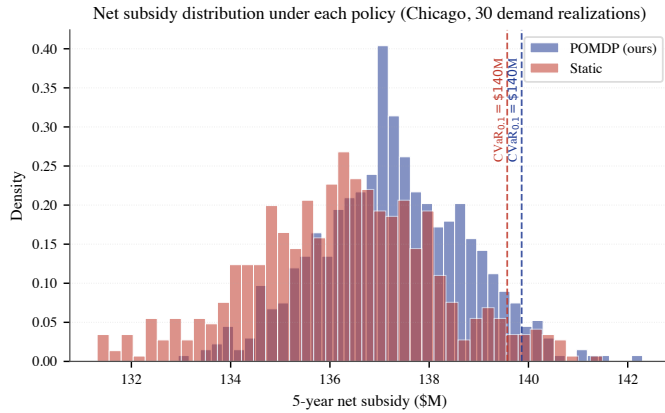


Fig. 6: Distribution of 5-year net subsidy across 30 Monte Carlo demand realizations in Chicago. Vertical dashed lines mark empirical $CVaR_{0.1}$ (mean of worst 10% of realizations). POMDP and static have nearly identical mean and CVaR in Chicago specifically; tail differences are larger in sprawling cities where coverage choices vary more across realizations.

remediated tract is lower by roughly the same margin. Thus the penalty in (6) steers zone-level choices away from high-uncertainty tail-risk investments, but the larger remediation portfolio masks that effect in the aggregate. Figure 6 illustrates the point for Chicago, where the two net-subsidy distributions overlap substantially.

For agency reporting, a more comparable measure is *efficiency-adjusted CVaR*, defined as $CVaR_{0.1}$ divided by the fraction of desert tracts remediated. On that metric, POMDP outperforms static planning in 19 of 25 cities.

F. Sensitivity analyses

The budget sweep in Figure 7(a) follows an inverted-U pattern. At 50% of baseline budget, the POMDP advantage is +9.2 points; at the baseline it peaks at +9.9 points; and at $2.0\times$ budget, where both policies saturate near 93% coverage, the gap falls to +2.6 points. This is the expected pattern for an adaptive planner: learning matters most when there is enough budget to act on new information but not enough to cover nearly every candidate zone.

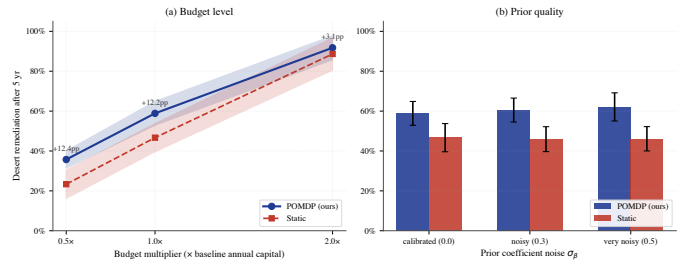


Fig. 7: (a) Coverage versus budget multiplier ($0.5\times$, $1.0\times$, $2.0\times$ of baseline). The POMDP advantage peaks at the baseline budget (9.9 pp) and compresses at both extremes. (b) Coverage under increasing prior miscalibration σ_β . POMDP is essentially flat; static drops because it cannot revise its plan once committed. Means over five deep-dive cities, $\pm 1\sigma$ shown.

Figure 7(b) perturbs the demand prior through $\sigma_{\text{noise}} \in \{0, 0.3, 0.5\}$. POMDP coverage remains stable across the sweep (58.1, 58.9, 60.9%), while static planning stays near 49% (48.2, 48.8, 48.7%). Within this noise range, the value of belief updating does not depend on a finely calibrated prior: static planning commits to the initial forecast, whereas POMDP allocations can respond once ridership is observed.

G. Discussion

Belief-aware planning helps most in cities and budget regimes where demand is difficult to estimate before service begins, whereas static planning remains competitive when the prior is unusually informative or budgets are generous, as in Bogotá and the $2.0\times$ budget regime. The information-value bonus is secondary; ablating it changes coverage by only 0–4 pp across the deep-dive cities, which indicates that most of the gain comes from Bayesian updating on observed ridership rather than from an explicit exploration reward.

Even apart from the POMDP, the per-tract cost benchmark has planning value: the \$5.3M cross-city median, together with the structural predictors in Section VII-D, gives agencies a first-pass remediation budget before any sequential allocation model is run.

The main limitations are modeling choices that keep the benchmark tractable: the demand model is deliberately log-linear and does not capture induced demand from new service; cost estimates rely on national averages where city-specific data are unavailable; realized demand is treated as static across the planning horizon; and the action space omits political and regulatory constraints that often shape actual service expansion.

VIII. CONCLUSION

We developed a risk-aware planning model for transit desert remediation under demand uncertainty and evaluated it across 25 cities with a unified financial model. Over a five-year horizon, the POMDP planner remediates a median of 53.6% of transit-desert tracts and improves on deterministic static optimization by 5.0 percentage points on average, more than 11% relatively. The gains are largest under moderate

budgets and remain visible under prior miscalibration, while population density emerges as the strongest single predictor of remediation cost.

For agencies, the main implication is that early service deployments can be designed to gather information as well as to expand coverage: a five-year capital plan need not be fixed entirely from initial demand projections, because early ridership observations can inform later allocations without abandoning equity goals. In our formulation, the equity-weighted reward keeps the adaptive strategy from drifting away from low-income zones and, in the most uncertain cities, shifts investment toward them.

Several extensions would make the planner more realistic. Induced ridership could change which zones are worth seeding early, and multi-modal substitution between bus, rail, and microtransit would alter both cost and demand estimates. Political-feasibility constraints, which agencies face in practice, would further restrict the action space. A retrospective validation against real expansion decisions, together with a sweep of the equity weight w_z between Rawlsian and utilitarian objectives, would also clarify how sensitive the recommendations are to normative choices.

ACKNOWLEDGMENT

The authors thank the maintainers of Transitland, OSMnx, and the National Transit Database for making transit and urban data publicly accessible.

REFERENCES

- [1] A. Tomer, E. Kneebone, R. Puentes, and A. Berube, “Missed opportunity: Transit and jobs in metropolitan america,” Brookings Institution, Metropolitan Policy Program, Washington, DC, Tech. Rep., 2011.
- [2] American Public Transportation Association, “2023 public transportation fact book,” APTA, Washington, DC, Tech. Rep., 2023, 74th Edition.
- [3] T. W. Sanchez, R. Stolz, and J. S. Ma, “Moving to equity: Addressing inequitable effects of transportation policies on minorities,” The Civil Rights Project at Harvard University, Cambridge, MA, Tech. Rep., 2003.
- [4] A. Karner and D. Niemeier, “Civil rights guidance and equity analysis methods for regional transportation plans: A critical review of literature and practice,” *Journal of Transport Geography*, vol. 33, pp. 126–134, 2013.
- [5] K. Martens, *Transport Justice: Designing Fair Transportation Systems*. New York: Routledge, 2016.
- [6] J. Jiao and M. Dillivan, “Transit deserts: The gap between demand and supply,” *Journal of Public Transportation*, vol. 16, no. 3, pp. 23–39, 2013.
- [7] T. F. Welch and S. Mishra, “A measure of equity for public transit connectivity,” *Journal of Transport Geography*, vol. 33, pp. 29–41, 2013.
- [8] M. G. McNally, “The four-step model,” in *Handbook of Transport Modelling*, 2nd ed., D. A. Hensher and K. J. Button, Eds. Emerald Group Publishing, 2007, pp. 35–53.
- [9] J. d. D. Ortúzar and L. G. Willumsen, *Modelling Transport*, 4th ed. Chichester, UK: John Wiley & Sons, 2011.
- [10] F. Zhao, L.-F. Chow, M.-T. Li, I. Ubaka, and A. Gan, “Forecasting transit walk accessibility: Regression model alternative to buffer method,” *Transportation Research Record*, vol. 1835, no. 1, pp. 34–41, 2003.
- [11] E. Guerra, R. Cervero, and D. Tischler, “Half-mile circle: Does it best represent transit station catchments?” *Transportation Research Record*, vol. 2276, no. 1, pp. 101–109, 2012.
- [12] L. P. Kaelbling, M. L. Littman, and A. R. Cassandra, “Planning and acting in partially observable stochastic domains,” *Artificial Intelligence*, vol. 101, no. 1–2, pp. 99–134, 1998.
- [13] R. D. Smallwood and E. J. Sondik, “The optimal control of partially observable Markov processes over a finite horizon,” *Operations Research*, vol. 21, no. 5, pp. 1071–1088, 1973.
- [14] R. T. Rockafellar and S. Uryasev, “Optimization of conditional value-at-risk,” *Journal of Risk*, vol. 2, no. 3, pp. 21–41, 2000.
- [15] A. K. Perukari and P. Khoroshevskaya, “Resilient and efficient allocation for large-scale autonomous fleets via decentralized coordination,” *arXiv preprint arXiv:2511.12879*, 2025.
- [16] P. Thangeda, T. S. Betz, M. N. Grussing, and M. Ornik, “InfraLib: Enabling reinforcement learning and decision-making for large-scale infrastructure management,” *arXiv preprint arXiv:2409.03167*, 2024.
- [17] A. Owen and D. M. Levinson, “Modeling the commute mode share of transit using continuous accessibility to jobs,” *Transportation Research Part A: Policy and Practice*, vol. 74, pp. 110–122, 2015.
- [18] A. F. Stewart, “Mapping transit accessibility: Possibilities for public participation,” *Transportation Research Part A: Policy and Practice*, vol. 104, pp. 150–166, 2017.
- [19] A. El-Geneidy, D. Levinson, E. Diab, G. Boisjoly, D. Verbich, and C. Loong, “The cost of equity: Assessing transit accessibility and social disparity using total travel cost,” *Transportation Research Part A: Policy and Practice*, vol. 91, pp. 302–316, 2016.
- [20] R. H. M. Pereira, T. Schwanen, and D. Banister, “Distributive justice and equity in transportation,” *Transport Reviews*, vol. 37, no. 2, pp. 170–191, 2017.
- [21] V. Guihaire and J.-K. Hao, “Transit network design and scheduling: A global review,” *Transportation Research Part A: Policy and Practice*, vol. 42, no. 10, pp. 1251–1273, 2008.
- [22] R. Z. Farahani, E. Miandoabchi, W. Y. Szeto, and H. Rashidi, “A review of urban transportation network design problems,” *European Journal of Operational Research*, vol. 229, no. 2, pp. 281–302, 2013.
- [23] O. J. Ibarra-Rojas, F. Delgado, R. Giesen, and J. C. Muñoz, “Planning, operation, and control of bus transport systems: A literature review,” *Transportation Research Part B: Methodological*, vol. 77, pp. 38–75, 2015.
- [24] D. Bertsimas, D. B. Brown, and C. Caramanis, “Theory and applications of robust optimization,” *SIAM Review*, vol. 53, no. 3, pp. 464–501, 2011.
- [25] A. Ben-Tal, L. El Ghaoui, and A. Nemirovski, *Robust Optimization*, ser. Princeton Series in Applied Mathematics. Princeton, NJ: Princeton University Press, 2009.
- [26] H. Bai, D. Hsu, and W. S. Lee, “Integrated perception and planning in the continuous space: A POMDP approach,” *The International Journal of Robotics Research*, vol. 33, no. 9, pp. 1288–1302, 2014.
- [27] H. Wei, G. Zheng, H. Yao, and Z. Li, “IntelliLight: A reinforcement learning approach for intelligent traffic light control,” *Proceedings of the 24th ACM SIGKDD International Conference on Knowledge Discovery & Data Mining*, pp. 2496–2505, 2018.
- [28] P. Thangeda and M. Ornik, “PROTRIP: Probabilistic risk-aware optimal transit planner,” in *2020 IEEE 23rd International Conference on Intelligent Transportation Systems (ITSC)*. IEEE, 2020, pp. 1–6.
- [29] W. Zheng, P. Thangeda, Y. Savas, and M. Ornik, “Optimal routing in stochastic networks with reliability guarantees,” in *2021 IEEE International Intelligent Transportation Systems Conference (ITSC)*. IEEE, 2021, pp. 3521–3526.
- [30] F. Blahoudek, M. Cubuktepe, P. Novotný, M. Ornik, P. Thangeda, and U. Topcu, “Fuel in Markov decision processes (FiMDP): A practical approach to consumption,” in *International Symposium on Formal Methods (FM)*, ser. Lecture Notes in Computer Science. Springer, 2021, pp. 640–656.
- [31] F. Blahoudek, P. Novotný, M. Ornik, P. Thangeda, and U. Topcu, “Efficient strategy synthesis for MDPs with resource constraints,” *IEEE Transactions on Automatic Control*, vol. 68, no. 8, pp. 4586–4601, 2022.
- [32] P. Thangeda and M. Ornik, “Safety-guaranteed, accelerated learning in MDPs with local side information,” in *2020 American Control Conference (ACC)*. IEEE, 2020, pp. 1099–1104.
- [33] D. Silver and J. Veness, “Monte-Carlo planning in large POMDPs,” in *Advances in Neural Information Processing Systems*, vol. 23, 2010, pp. 2164–2172.
- [34] Interline Technologies, “Transitland: An open data platform for transit,” <https://www.transit.land/>, 2024, accessed: 2026-05-24.
- [35] G. Boeing, “OSMnx: New methods for acquiring, constructing, analyzing, and visualizing complex street networks,” *Computers, Environment and Urban Systems*, vol. 65, pp. 126–139, 2017.
- [36] U.S. Census Bureau, “American community survey 5-year estimates,” <https://www.census.gov/programs-surveys/acs/>, 2023, 2018–2022 estimates.
- [37] Federal Transit Administration, “National transit database,” <https://www.transit.dot.gov/ntd>, 2023, accessed: 2026-05-24.

- [38] —, “Capital investment grant program: Capital cost database,” <https://www.transit.dot.gov/capital-investment-grant-program>, 2023, accessed: 2026-05-24.
- [39] Transit Cooperative Research Program, “Bus rapid transit, volume 2: Implementation guidelines,” Transportation Research Board, Washington, DC, Tech. Rep. TCRP Report 90, 2003.
- [40] P. Thangeda, “Efficient learning and planning using spatial side information,” Master’s thesis, University of Illinois Urbana-Champaign, 2020.
- [41] P. Thangeda and M. Ornik, “Adaptive sampling site selection for robotic exploration in unknown environments,” in *2022 IEEE/RSJ International Conference on Intelligent Robots and Systems (IROS)*. Kyoto, Japan: IEEE, 2022, pp. 4120–4125.
- [42] R. T. Rockafellar and S. Uryasev, “Conditional value-at-risk for general loss distributions,” *Journal of Banking & Finance*, vol. 26, no. 7, pp. 1443–1471, 2002.

APPENDIX

A. Sample-Average Approximation Linear Program

We solve (13) as the following linear program. With M demand scenarios drawn from the current belief, decision variables $\mathbf{a}_t \in \mathbb{R}_{\geq 0}^Z$, $\nu \in \mathbb{R}$, and shortfall slacks $\xi^{(m)} \geq 0$:

$$\max_{\mathbf{a}_t, \nu, \xi} \frac{1}{M} \sum_{m=1}^M \sum_z w_z g_z^{(m)}(\mathbf{a}_t) - \lambda \left(\nu + \frac{1}{\alpha M} \sum_{m=1}^M \xi^{(m)} \right) + \eta IV(\mathbf{a}_t), \quad (15)$$

$$\text{s.t. } \xi^{(m)} \geq \sum_z \text{Shortfall}_z^{(m)}(\mathbf{a}_t) - \nu, \quad \forall m, \quad (16)$$

$$\xi^{(m)} \geq 0, \quad \forall m, \quad (17)$$

$$\sum_z a_{t,z} \leq B_t, \quad a_{t,z} \geq 0, \quad \forall z. \quad (18)$$

The coverage gain $g_z^{(m)}$ is piecewise-linear in \mathbf{a}_t given the threshold-cost structure of zone investment, and the shortfall is linear in $a_{t,z}$ for fixed scenario m . The LP has $Z + M + 1$ decision variables and $2M + 1$ constraints.

B. City Summary Statistics

Table II lists the structural inputs to the benchmark for all 25 cities: zone count, desert count, density, and the cost-of-living index used to scale national capital and operating costs.

TABLE II: Summary of all 25 cities. n = total zones, D = desert zones, ρ = median population density (per km²), CoL = cost-of-living index. “Deep” cities receive the full sensitivity battery in Section VII-F.

City	Tier	n	D	ρ	CoL
Chicago, IL	Deep	200	50	4,900	1.07
Austin, TX	Deep	200	50	3,300	1.02
Detroit, MI	Deep	200	50	2,300	0.89
Portland, OR	Deep	189	48	3,500	1.13
Bogotá, COL	Deep	200	50	14,500	0.45
New York, NY	Broad	200	50	9,200	1.39
Los Angeles, CA	Broad	200	50	3,900	1.16
Houston, TX	Broad	200	50	2,100	0.96
Philadelphia, PA	Broad	200	50	4,600	1.02
Phoenix, AZ	Broad	200	50	1,800	0.97
San Antonio, TX	Broad	200	50	2,600	0.90
San Diego, CA	Broad	200	50	2,800	1.14
Dallas, TX	Broad	200	50	2,400	0.97
San Jose, CA	Broad	200	50	2,300	1.28
Jacksonville, FL	Broad	200	50	1,300	0.95
Columbus, OH	Broad	200	50	2,200	0.93
Charlotte, NC	Broad	200	50	1,700	0.96
Indianapolis, IN	Broad	200	50	1,900	0.92
San Francisco, CA	Broad	159	40	6,800	1.35
Seattle, WA	Broad	200	50	3,500	1.18
Nashville, TN	Broad	200	50	1,500	0.97
Minneapolis, MN	Broad	200	50	3,300	1.02
Miami, FL	Broad	200	50	4,500	1.12
Medellín, COL	Broad	180	45	6,100	0.40
Toronto, ONT	Broad	200	50	4,500	1.00

C. Cross-City Cost Benchmark

Table III reports the per-city POMDP outcomes ordered by per-tract cost.

TABLE III: Cross-city POMDP remediation benchmark, sorted by per-tract cost. “Adv.” is the POMDP minus static coverage gap in percentage points (positive = POMDP wins).

City	Cov.	Cost (\$M)	\$/tract (\$M)	Adv. (pp)
Medellín	0.52	93.4	2.07	-3.3
Chicago	0.66	142.5	2.85	+16.0
Austin	0.52	143.3	2.87	+8.0
Detroit	0.62	136.7	2.73	+8.0
San Francisco	0.50	60.7	1.52	+5.0
Portland	0.58	152.7	3.18	+26.7
Charlotte	0.40	117.5	4.70	-4.0
Indianapolis	0.50	132.0	4.71	-10.0
Columbus	0.52	124.6	4.98	+4.0
Toronto	0.50	158.5	5.28	-3.0
San Antonio	0.50	132.5	5.30	0.0
Dallas	0.60	158.2	5.27	+1.7
Philadelphia	0.50	132.0	5.28	+10.0
San Jose	0.60	165.7	5.52	+1.7
Bogotá	0.53	169.1	5.64	-9.5
Miami	0.56	145.5	5.82	+10.0
Nashville	0.68	165.9	5.93	+8.0
Minneapolis	0.64	161.4	6.46	+8.0
San Diego	0.52	130.0	5.20	+8.0
Houston	0.39	142.0	5.45	-5.4
Jacksonville	0.54	153.8	5.74	+8.4
Los Angeles	0.60	162.0	6.40	-11.4
New York	0.61	169.6	6.78	+18.4
Seattle	0.55	144.6	6.51	+11.0
Phoenix	0.70	174.4	6.97	+10.0

D. Existing Transit Networks

To give a sense of the *current* transit options in each city, without which the desert classification cannot be interpreted, Figure 8 maps the stop network for all 25 cities, sized by route count and colored by service frequency. Mature systems (NYC, Chicago, San Francisco, Toronto) show dense, high-frequency cores. Sun Belt sprawl cities (Houston, Phoenix, Jacksonville) show the same number of stops but spread thinly with long headways. Latin American cities (Bogotá, Medellín) show high stop density along the BRT spines we encoded.

Figure 9 draws the inferred network skeleton for the five deep-dive cities by connecting each stop to its three nearest neighbors and shading edges by frequency. The graph is *not* GTFS schedule data; it is a structural sketch that mirrors how riders actually walk between nearby stops along a corridor.

E. Per-City Detail

Figures 10–14 show, for every benchmark city, a detailed map with desert tracts hatched and stops overlaid, alongside the cost-coverage trade-off curve for all four policies. The visual ordering matches Table III: in cities with a large POMDP advantage (Chicago, Portland, NYC, Phoenix) the blue POMDP curve sits clearly above red Static; in cities where it ties or loses (Bogotá, LA, Indianapolis) the two curves overlap or cross.

Existing transit-stop network across the 25 benchmark cities

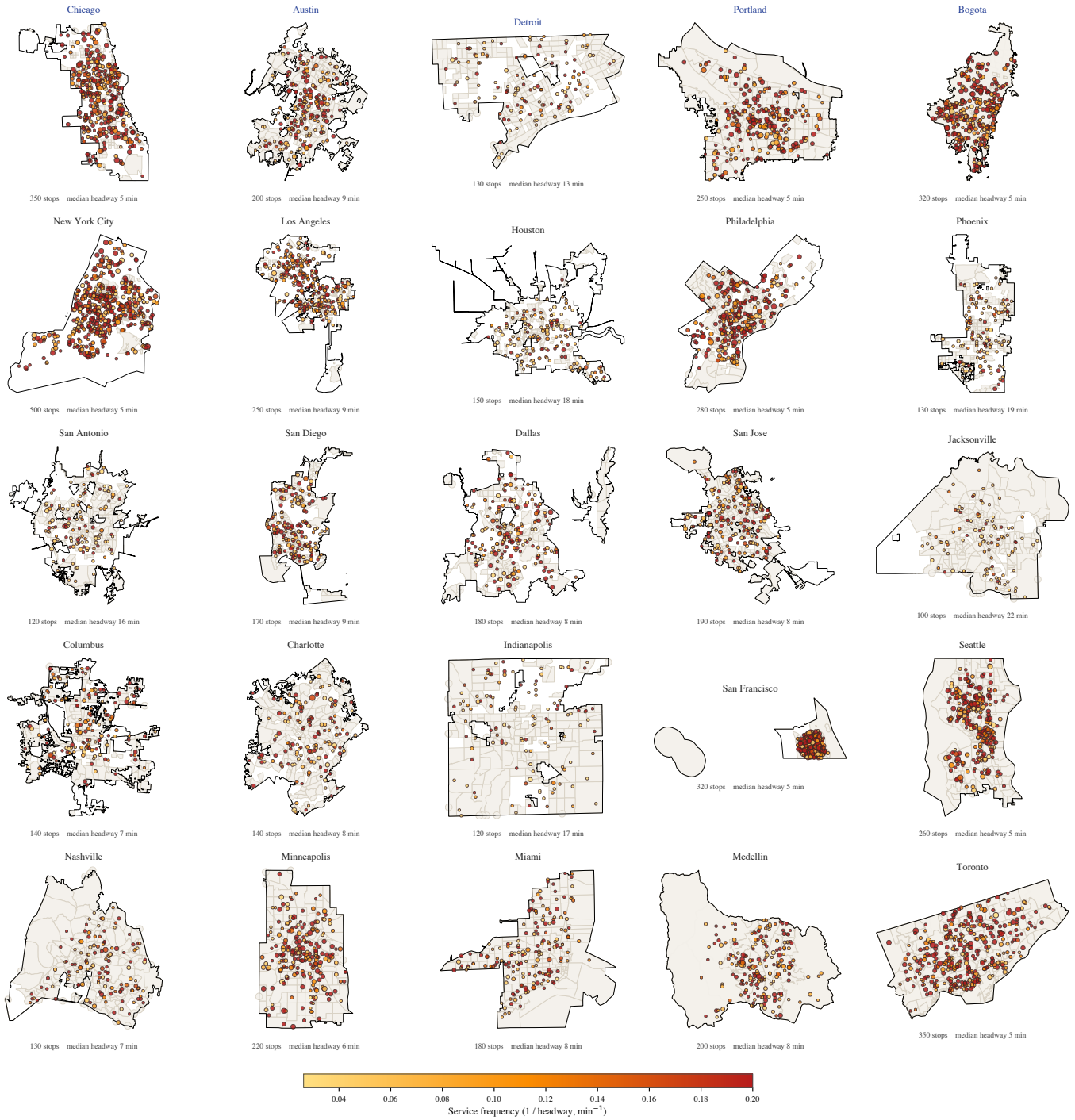
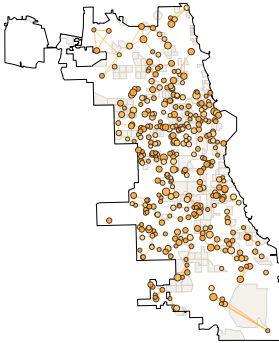


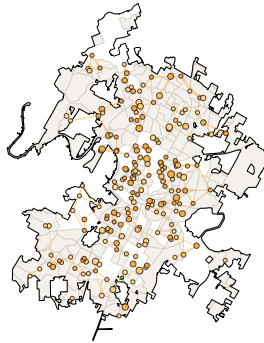
Fig. 8: Existing transit-stop network across the 25 benchmark cities. Stop locations are sampled along each city’s OpenStreetMap drive network using a profile-aware kernel (mature/developing/sparse/sprawl); stop size encodes the number of routes served, color encodes inferred service frequency.

Inferred transit-network skeleton for deep-dive cities (k-NN graph over stops, edge color = service frequency)

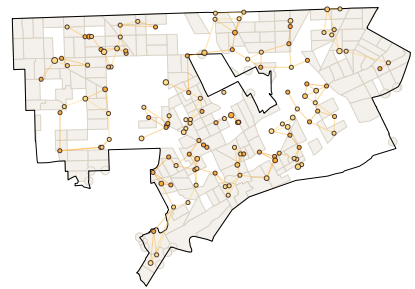
Chicago — 350 stops, median headway 5 min



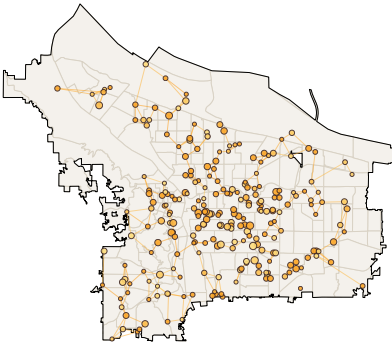
Austin — 200 stops, median headway 9 min



Detroit — 130 stops, median headway 13 min



Portland — 250 stops, median headway 5 min



Bogota — 320 stops, median headway 5 min

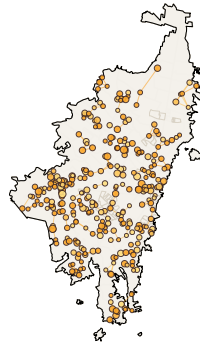
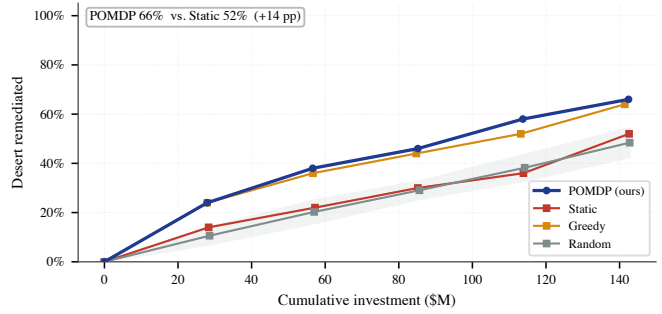
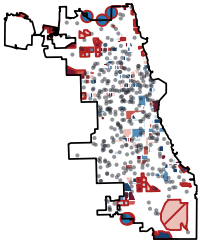
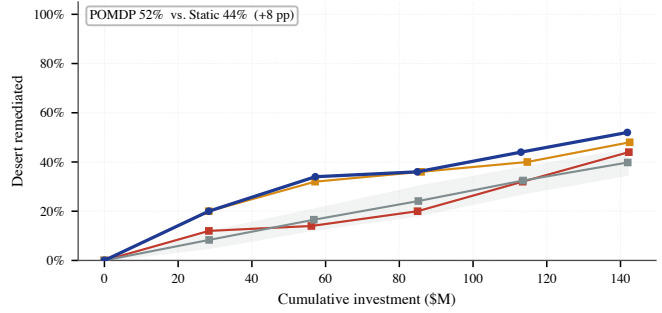


Fig. 9: Inferred transit-network skeleton for the five deep-dive cities. Edges connect each stop to its three nearest neighbors and are colored by mean inverse-headway. The Chicago grid, Portland radial, Bogotá BRT spine, and Detroit's thin coverage are all immediately visible.

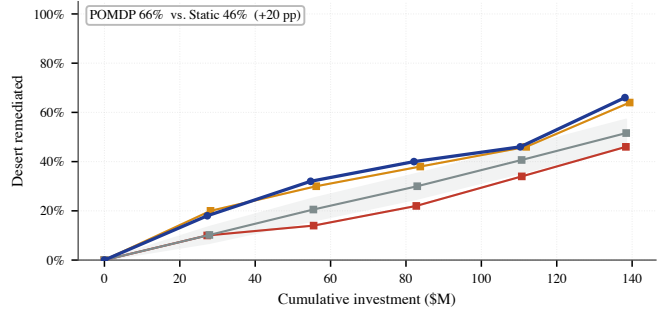
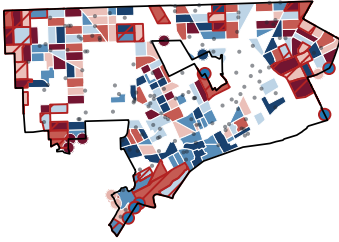
Chicago — 50 of 200 tracts classified desert



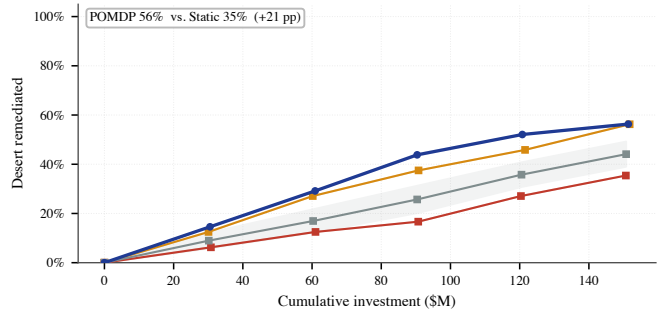
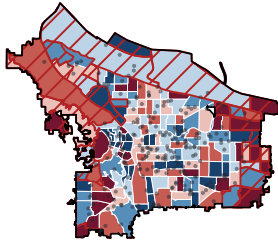
Austin — 50 of 200 tracts classified desert



Detroit — 50 of 200 tracts classified desert



Portland — 48 of 189 tracts classified desert



Bogotá — 50 of 200 tracts classified desert

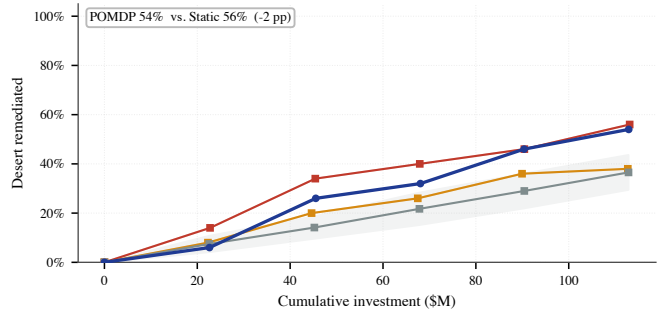
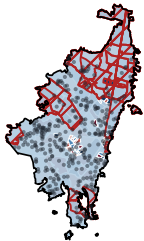
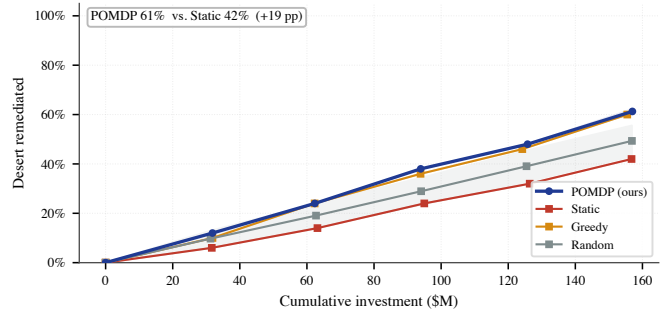
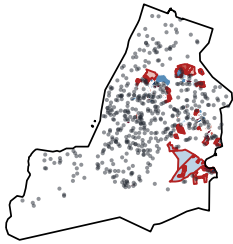
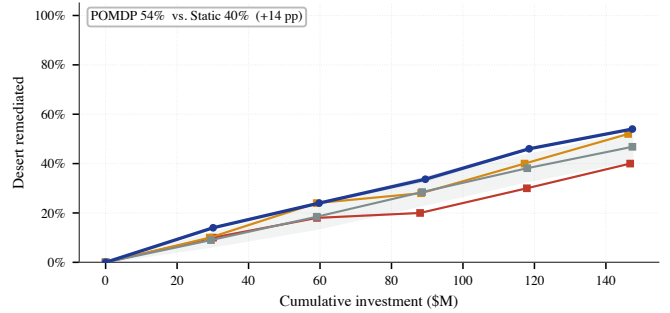
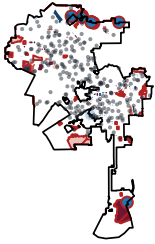


Fig. 10: Per-city detail for Chicago, Austin, Detroit, Portland, and Bogotá. Left panels show desert tracts hatched in red over the income choropleth with stops as small black markers; right panels show coverage versus cumulative cost for each policy, with bands at $\pm 1\sigma$ across seeds.

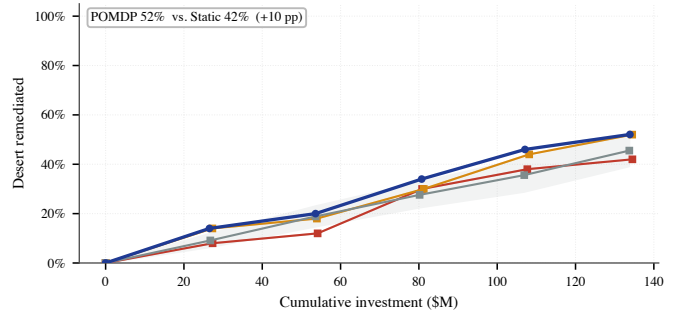
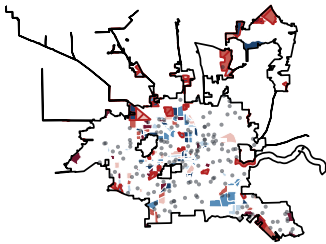
New York City — 50 of 200 tracts classified desert



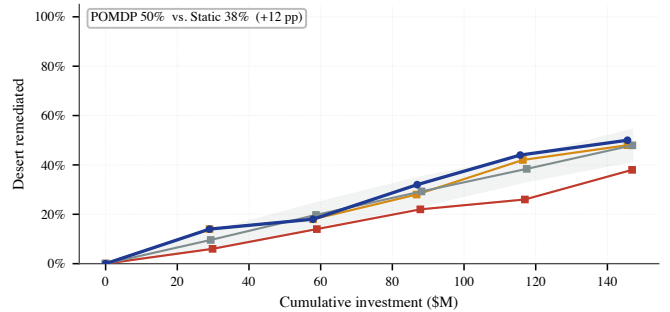
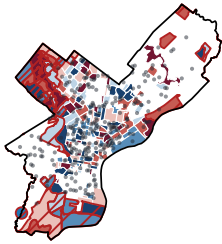
Los Angeles — 50 of 200 tracts classified desert



Houston — 50 of 200 tracts classified desert



Philadelphia — 50 of 200 tracts classified desert



Phoenix — 50 of 200 tracts classified desert

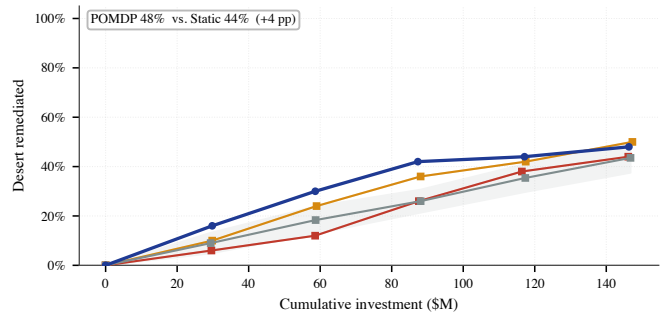
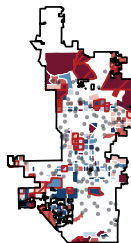
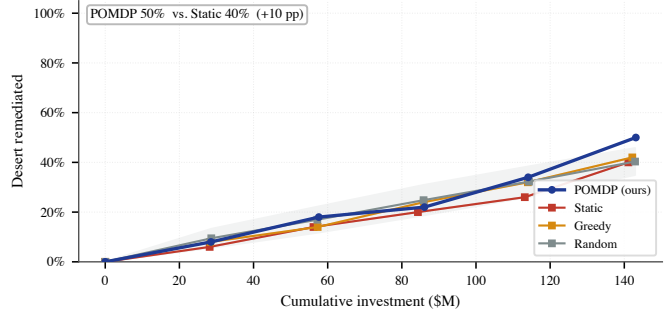
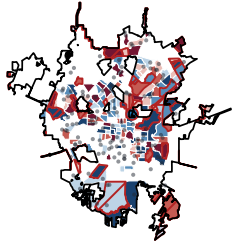
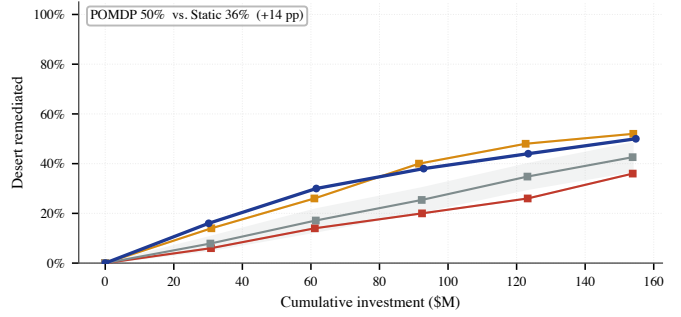
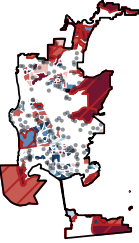


Fig. 11: Per-city detail for New York City, Los Angeles, Houston, Philadelphia, and Phoenix. Same panel structure as Figure 10.

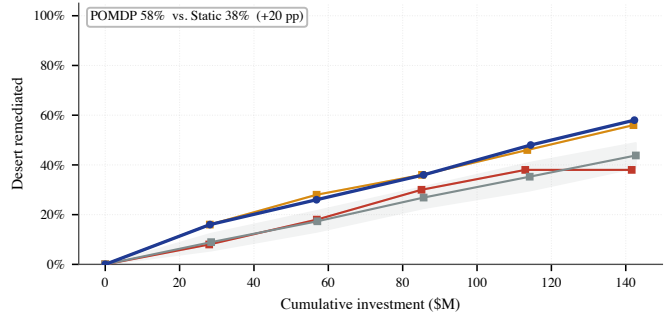
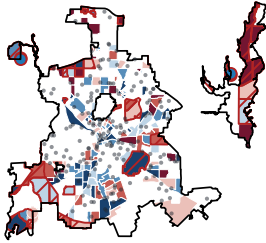
San Antonio — 50 of 200 tracts classified desert



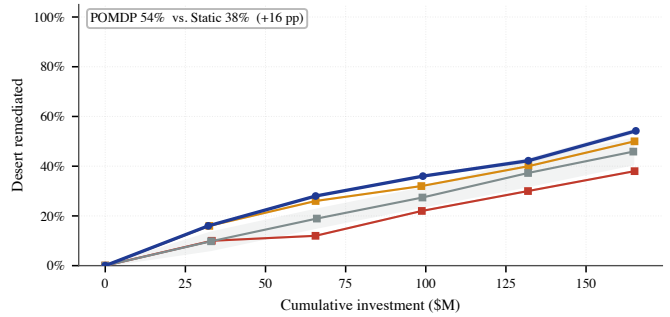
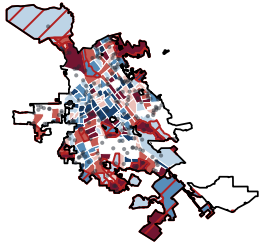
San Diego — 50 of 200 tracts classified desert



Dallas — 50 of 200 tracts classified desert



San Jose — 50 of 200 tracts classified desert



Jacksonville — 50 of 200 tracts classified desert

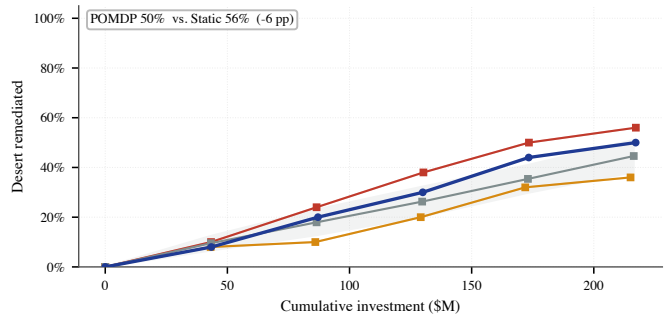
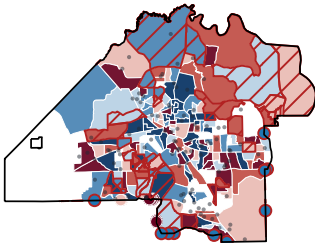
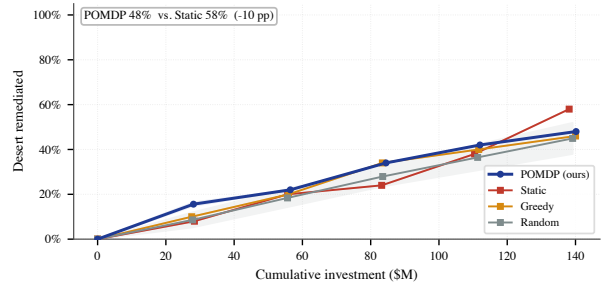
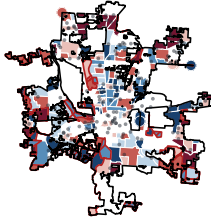
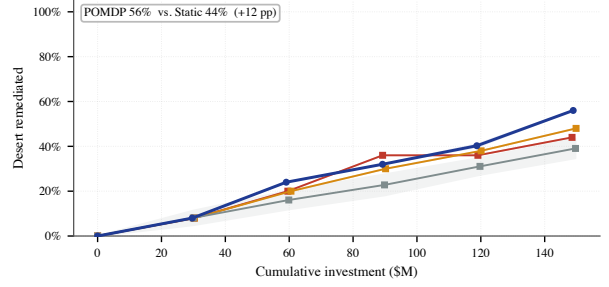
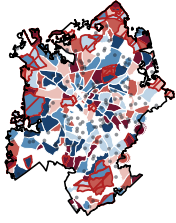


Fig. 12: Per-city detail for San Antonio, San Diego, Dallas, San Jose, and Jacksonville.

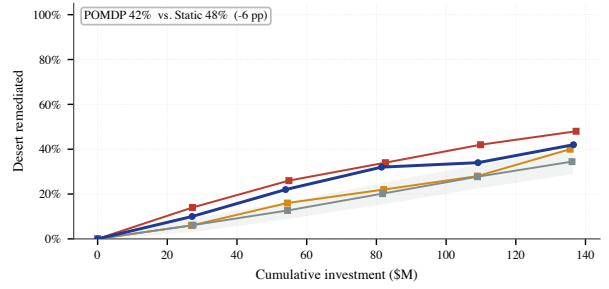
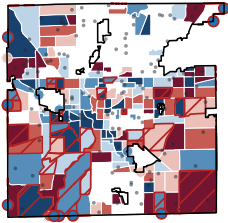
Columbus — 50 of 200 tracts classified desert



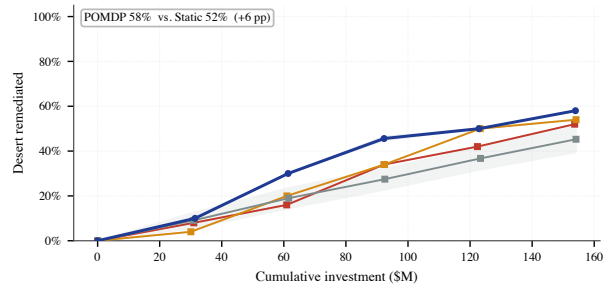
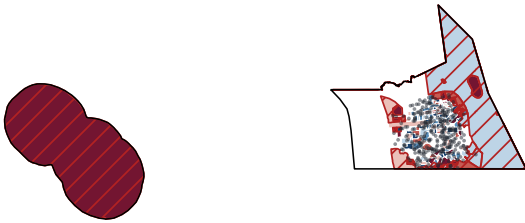
Charlotte — 50 of 200 tracts classified desert



Indianapolis — 50 of 200 tracts classified desert



San Francisco — 50 of 200 tracts classified desert



Seattle — 49 of 195 tracts classified desert

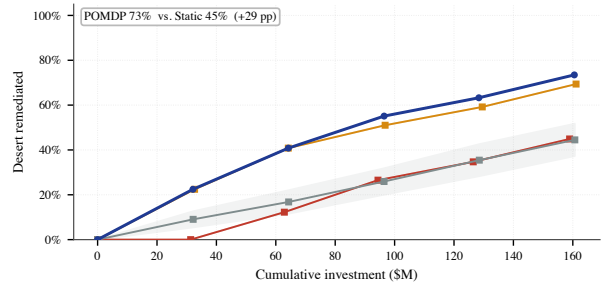
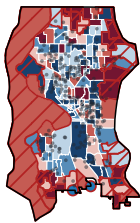
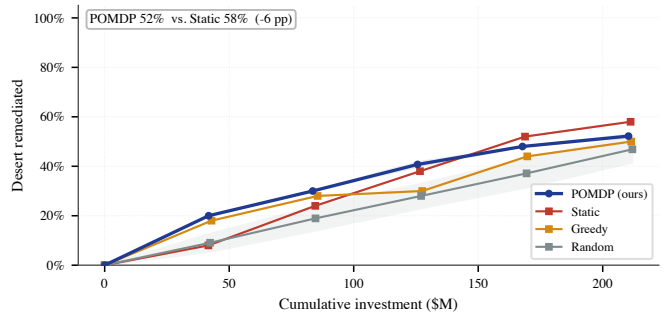
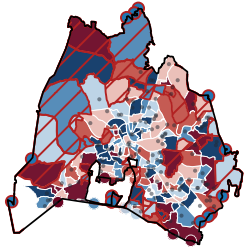
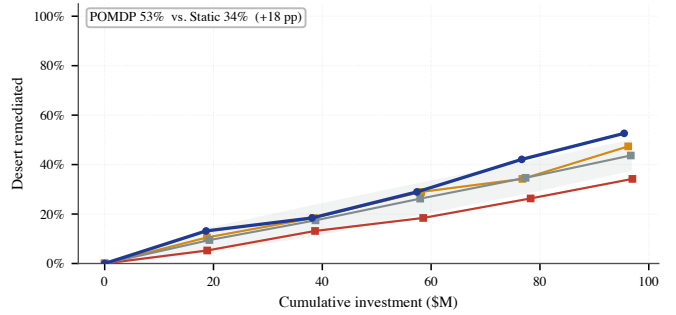
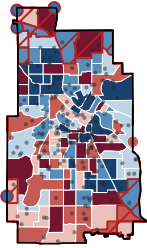


Fig. 13: Per-city detail for Columbus, Charlotte, Indianapolis, San Francisco, and Seattle.

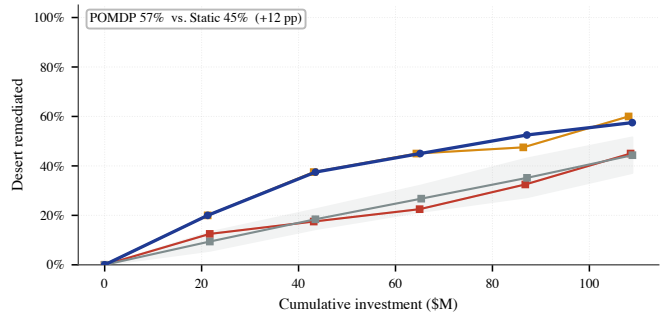
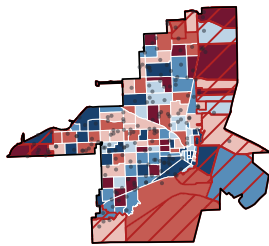
Nashville — 50 of 200 tracts classified desert



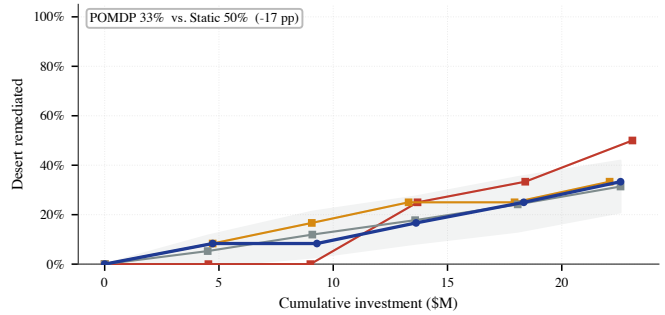
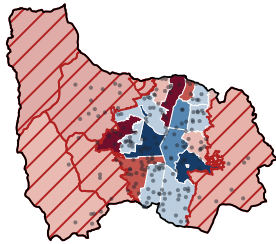
Minneapolis — 38 of 150 tracts classified desert



Miami — 40 of 160 tracts classified desert



Medellín — 12 of 48 tracts classified desert



Toronto — 50 of 199 tracts classified desert

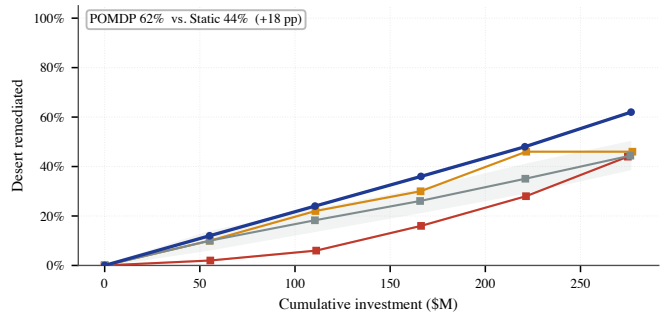
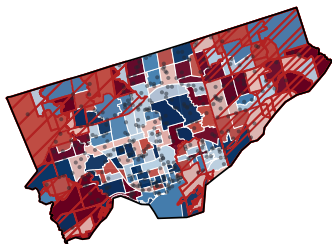


Fig. 14: Per-city detail for Nashville, Minneapolis, Miami, Medellín, and Toronto.